Bulletin of Electrochemistry 17 (4) April 2001, pp 183-192

0256-1654/2001/$ 3-50

Critical Review on ELECTROCHEMICAL QUARTZ CRYSTAL MICRO BALANCE — PRINCIPLES AND APPLICATIONS TO CORROSION RESEARCH

V S MURALIDHARAN

Central Electrochemical Research Institute, Karaikudi 630 006. INDIA

INTRODUCTION

In 1880, Jacques and Pierre Curie discovered that when mechanical stress was applied to the surface of various crystals like Quartz, rochelle salt and Tourmaline, an electrical potential was developed. The magnitude was proportional to the applied stress. This effect is known as Piezo electric effect. The Greek word 'Piezin' means. "to press" [1].

The piezo electric effect is seen on crystals of eccentric materials. These materials crystallise into non centro symmetric space groups and their single crystal possess a polar axis. This polar axis is due to the dipoles associated with the arrangement of atoms in the crystalline lattice. Under mechanical stress a quartz crystal generates a charge. This is due to the change in the dipole moment arising from the physical displacement of atoms. The magnitude and direction of the electric charge depends on the relative orientation of the dipoles and the crystal faces.

Conversely the application of a potential across these crystals resulted in a corresponding mechanical strain. This is the principle underlying the operation of EQCM. [Electro Chemical Quartz Micro balance].

Quartz Crystals

Natural crystal has the shape of a hexagonal prism with a pyramid attached to each end [Fig. 1]. The line joining the end points of these pyramids which pass through the opposite corners of the crystal constitute its 3 X-axis or electrical axes and of the hexagon form its 3 Y-axis or mechanical axes. Thin plates cur perpendicular to X-axes are called X-cut plates which can generate longitudinal mode of ultrasonic vibrations where as those cut perpendicular Y-axes are known as Y-cut plates which generate transverse mode of vibrations. For example a X-cut crystal plate of thickness "t" and length "1" its thickness is parallel to X-axis, the length is parallel to Y-axis and the breath is parallel to Z-axis [2].

For QCM applications, the AT, BT, and SC [stress compensated] cuts have been used [3]. At refers to the orientation of the crystal with respect to its large faces, this particular crystal is fabricated by slicing through a quartz rode at an angle of

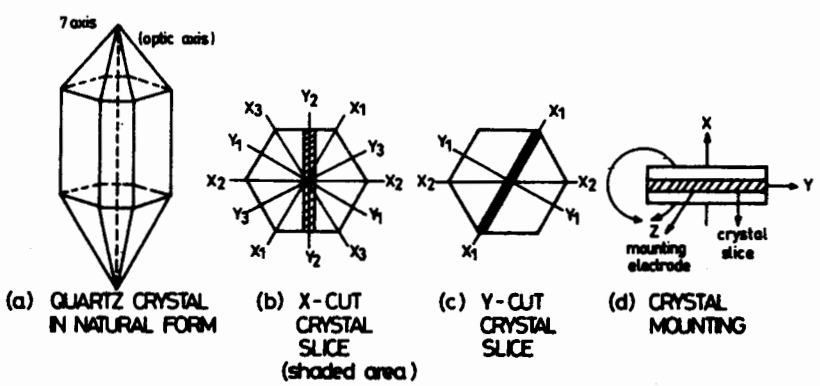

Fig. 1: Preparation of piezoelectric crysal

approximately 35 degrees with the crystallographic X-axis. The AT cut quartz crystals are particularly popular because they can be cut to give nearly zero temperature coefficient at one or more temperatures. However temperature effects for crystals immersed in liquids far out weigh the intrinsic temperature dependence of the crystals themselves and they must be taken into account. SC cut crystals would seem to offer certain advantages in terms of the elimination of the stress induced frequency changes. The AT cut crystals are covered with thin metal electrode pads. The electrode pads kept on the opposite sides of the crystal overlap in the centre of the crystal with tabs extending from each to the edge of the crystal where electrical contact is made. For mass measurements plane and plano-convex AT cut crystals are used.

When an electrical potential is applied, across the crystal using these electrode, the AT cut crystal experiences a mechanical strain in the shear direction. Crystal symmetry dictates that the strain induced in a piezo electric material by an applied potential of one polarity will be equal and opposite in direction to that resulting from the opposite polarity. Therefore an alternating potential across the crystal causes vibrational motion of the quartz crystal with vibrational amplitude parallel to the crystal surface and the X-direction. This oscillatory behaviour and the electrochemical "Micro Generator" properties are basis of a myraid of applications.

Quartz chemical mass

QCM crystals are typically employed as thin shaped transducers which oscillate in a pure shear mode when an alternating electric field of the proper frequency is applied across the disk. This means that the electric field lines are normal to the disk surface. The motion of the disk surface is precisely parallel to the disk face. Typical frequencies for these oscillations in QCMs are from 1 to 10 Mc/s. By proper design of the crystal other modes of vibrations can be eliminated [4].

The resonant frequency of the crystal may be identified as the frequency of maximum displacement of the crystal surface [For constant driving voltage]. This condition corresponds to the establishment of a standing acoustic wave within the bulk of the crystal with a node existing in the centre of the disk and the antinodes at the two surfaces. The resonant frequency can be seen to be related to the thickness of the crystal through the equation.

$$t_q = \frac{V_q}{2f_0} = \frac{\lambda_q}{2} \qquad (1)$$

where V_q is the velocity of the acoustic wave in quartz, f_0 is the resonant frequency, λ_q is the wave length of the acoustic wave in quartz. For an AT crystal V_q = 3340 m/s, t_q = 334 μM, t_q = 668 μM and f_0 = 5 MHZ.

The critical dimensions are the thickness of the quartz disk [t_q], the diameter of the crystal [d c] and the diameter of the concentric electric pad [de]. For a ratio of $d_c / t_q > 50$, unwanted modes may be suppressed by 40 dB. For a crystal the minimum d c for a 5 MHZ [t_q = 0.03 cm] is 1.5 cm and the minimum value is 0.54 cm. This calculations do not take into consideration the "flag" which extends from the edge of the circular part of the electrode to the edge of the crystal disk, but it has generally been found the flag has minimal influence on oscillator stability.

The problem of coupling to unwanted modes or to the structure used to mount the crystal is considered using the concept of energy trapping [5]. Energy trapping refers to the fact that most of the energy contained in the mechanical oscillation of the crystal if the region has a resonant frequency which is significantly lower than that of the non electroded region. This can be easily achieved by using rather thick [100 nM] or by contouring one or both faces of the crystal disk so that the thickness of the electroded region is significantly different from that of the rest of the disk.

Plane AT cut crystals have both disk surfaces parallel to within one μM depending on the manufacturer. Planoconvex crystals have one side of the disk flat and the other ground to have a very slight radius of curvature. A typical range of radius of curvature for a 1 inch diameter, 5 MHZ crystal would be 10- 50 cm. For planoconvex crystals the region of the crystal which undergoes displacement during the oscillation is confined completely to the area defined by the electrodes [or by the smaller of the two electrodes if they have different sizes]. For plane crystals this region extends some what past the edge of the electrode, onto the face of the quartz disk itself. The degree of extension of this region depends on the total mass loading of the crystal with this displacement being more completely confined to that part of the

crystal sandwiched between the electrodes fro higher loading [4-6]. For AT cur crystals operating in the frequency mode, the range of amplitutidues reported is 10-100 nM. The distribution of the vibrational amplititudes a function of radial distance from the centre of the electrode is also known. The amplitude is maximum in the centre of the disk and decays in an apparently Gaussian fashion with distance nearly reaching zero at the edge of the electrode. This Gaussian distribution becomes considerably sharper for plano-complex crystals as the radius of curvature is decreased or with increasing harmonic number. For a Mc/s crystal operating in the functional mode, the radial distance at which the amplitude is 1/e of its maximum value decreases by 30% when the radius of curvature is decreased from 50 to 6 cm. For a crystal having a radius of curvature of 10cm, this distance is decreased by 50% when the crystal is operated in its 3rd harmonic mode [12 MHZ] as opposed to the fundamental mode [4 MHZ]. For plano-convex crystals operated in the 3rd harmonic, the vibrational amplitude can be considered to be essentially zero at the edge of the electrode. For plane crystals operated in the fundamental mode in vacuum or in a low density gaseous environment, the amplitude distribution is known to be more confined to the electrode area as mass loading is increased.

The mass sensitivity is intimatelly related to the vibrational amplitude distribution. The different mass sensitivity $C_f = d_f / d_m$ and is a function of radial distance from the centre while the integrated mass sensitivity, C_f is shown to change slightly at small loading and then become relatively constant for larger loading $C_f = \int C_f \, dA$ where A is the area of the vibrational displacement. The vibrational motion of the quartz results in a transverse acoustic wave that propagates back and forth across the thickness of the crystal between the crystal faces. In the quartz resonator a standing wave condition is established when the acoustic wave length is equal to twice the combined thickness of the crystal and electrodes. The frequency of the acoustic wave fundamental mode

$$f_0 = \frac{vtr}{2t_q} \qquad (2)$$

vtr = Transverse velocity of sound in AT cut crystal = 3.34 x 10 4 m/s, t_q = Resonator thickness

The velocity of sound in quartz and in electrode is assumed to be identical. The acoustic velocity is dependent on the modulus and density of the crystal. The quartz crystal surface is at an antinode of the acoustic wave and the the wave propagates across the interface between the crystal and a foreign layer on its surface. If it is assumed that the acoustic wave velocity and the density of the foreign layer on its surface. If it is assumed that the acoustic wave velocity and the density of the foreign layer are identical to those in quartz a change in thickness of the foreign layer is tantamount to a change in the thickness of the quartz crystal. A fractional change in thickness results in a fractional change in the resonant frequency.

The well known Sauerbery equation is

$$\Delta f = \left(\frac{-2 f_0^2 \Delta m}{A (\mu_q p_q)^{1/2}} \right) \qquad (3)$$

where Δf = measured frequency change; f_0 = Frequency of the quartz resonator prior to a mass change; Δm = mass change; A = piezo electricity active area; P_q = Density of quartz [2.648 g/cc]; μ_q = Shear modulus of the AT cut quartz = 2.947×10^{11} dyne/sq.cm

This equation is the primary basis of the most QCM measurements where in mass changes occurring at the electrode interface are evaluated directly from the frequency changes of the quartz resonator. As long as thickness of the film added to QCM is < 2% of the quartz crystal thickness, this equation is valid. Deviations from Sauerbery equation due to higher mass loadings may be compensated by the use of the Z-match method. Though this method has been used for vacuum applications, it has yet to be employed in EQCM. For EQCM operating frequencies are 5 to 10 MHZ and these provide mass detection limits of 1 ng/sq.cm.

$$\Delta_f = -C_f \Delta m \qquad (4)$$

This negative sign shows that increase in mass corresponds to a decrease in frequency.

Lu and Lewis [8] gave an simple equation for dependence of Δf} on Δm

$$\tan \frac{\pi f_c}{f_0} = \frac{z_f}{z_q} \tan \frac{\pi f_c}{f_f} \qquad (5)$$

where f_c is the resonant frequency of the composite resonator formed from the crystal and the films present at the surface, f_f can be thought of as the resonant frequency of the free standing foreign film and Z_f and Z_q are the acoustic impedance of the film and quartz respectively.

$$\Delta f = f_c - f_0;\ f_f = \frac{V_f}{2t_f} = \frac{V_f P_f}{2\Delta m} \qquad (6)$$

$$V_f = \left(\frac{\mu_f}{P_f}\right)^{1/2};\ V_q = \left(\frac{\mu_q}{P_q}\right)^{1/2} \qquad (7)$$

$$Z_q = P_q V_q = (P_q\ \mu_q)^{1/2} \qquad (8)$$

$$Z_f = P_f V_f = (P_f\ \mu_f)^{1/2} \qquad (9)$$

where $t_f = \frac{\Delta m}{\mu_f}$; $\mu_q = 2.947 \times 10^{11}$ g/cm/sec^2; μ_g, μ_f are the shear moduli of quartz and the film respectively. The shear moduli of quartz is 2.947 x 10^{11} g/sq.sec/cm. P_f is the density of the film V_q, V_f are the velocities of the acoustic waves in the quartz and the film respectively. This analysis of frequency changes using the acoustic impedances of the quartz and the film is usually called the Z-match method.

Z-match method requires that the shear modulus of the deposit be known. If the density of the deposit is known, the Z-of the deposit may be obtained by assuming that its shear modulus is the same as that of quartz.

$$\tan \frac{\pi f_0}{f_0} = \frac{Z_f}{Z_q} \tan \frac{\pi f_0}{f_f} \qquad (10)$$

Using the above equation, the measurement of the change in resonant frequency at more than one frequency [usually the fundamental and third harmonics] provides a method for obtaining Z_f. This method requires the use of an oscillator that can be easily switched between operation at the fundamental and third harmonic frequencies or the use of an impedance analyser which can operate at a frequency high enough to measure the parameters of interest at the third harmonic.

A comparison of quartz crystal with other vibrating bodies is useful. For example in the case of vibrating string, a pendulum or a mass spring, the amplitude is defined by the initial energy input and the resonant frequencies are by the characteristics of mass and length. The motion of the quartz crystal is described as moving about X=0, rest point between the limits of -X max and +X max. The magnitude of X max will depend on he applied A.C voltage across the crystal. The potential energy of the crystal is at a maximum at X = ± X max, where as the kinetic energy is at a maximum at X = 0. The effect of mass or thickness changes on the quartz crystal resonant frequency can be understood by analogy to a spring balance. Standing wave conditions exist if their wavelengths are integral divisors of 2 l where l is the length of the string. The fundamental frequency, f_0 is given by

where S is the tension on the string and M is the mass per unit length. In the case of a spring balance an increase of mass of the string or its length result in a decrease in f_0. For an increase of thickness, the quartz crystal results in decrease of frequency.

During oscillation a pendulum may lose a considerable energy during oscillation because of friction. A quartz crystal may lose only a minute amount due to phonon interactions that produce heat, vibrational damping by the mounting components and acoustical losses to the environment. The ratio of the energy stored to energy lost during a single oscillation is characterised by the quality factor Q. For quartz crystal, Q is > 100000. The frequency of a typical quartz crystal can be determined to an accuracy of 1 part in 10^8. In liquids Q values for quartz crystals are 1000 to 3000 indicative of energy damping by the fluid.

Mechanical model of QCM

The resonance of a quartz crystal is explained with elements like mass, friction and compliance. Compliance is the ability of the resonator to yield elastically under an applied force. The equivalent circuit is the inductor, L1 representing the mass displaced during oscillation, C1, the energy stored during oscillation; The compliance is the inverse of the elastic or Hooke's constant. R1 is the energy dissipation due to losses that are tantamount to internal friction. An accurate description must include a parallel capacitor to represent the static capacitance of the quartz plate with its electrodes and any stray parasitic capacitances. The Butterworth-Van Dyke circuit [see Fig. 2] is used to represent this. The series branch is known as Motional branch as it reflects the vibrational branch. This LCR branch is identical to a tank circuit in which oscillations can be cycling of current between the capacitor and the inductor.

When the capacitor in this circuit discharge through the inductor, a magnetic field is established around the inductor as it opposes the current. When the capacitor discharge is complete and the current falls to zero. the electromotive force in the inductor creates a current in the direction opposite to the original current and the capacitor recharges. Repetition of this cycle results in electrical oscillation with oscillation damped by an amount proportional to R. I n the case of quartz crystals, the R values are rather small and sustained oscillations are favoured.

BVD circuit accurately describes the operation of QCM in vacuum or the gas phase, it is not applicable to liquids where the density and viscosity play a part. The density of the liquid adds to the mass of the resonator while its viscosity provides additional energy damping. The addition of extra inductance and resistance [L2,R2] in series with the motional branch of the BVD circuit takes into account the effect of extra mass and viscosity. At the liquid boundary the vibration causes a shear wave and it decays as an exponentially damped Cosine function [11-13].

$$V_x (Z,t) = Ae^{-kz} \cos (kZ - wt) \qquad (11)$$

where k is the propagation constant, Z is the distance from the resonator surface, A the maximum amplitude of the shear wave, w is angular frequency. The inverse of the propagation constant k is the decay length δ. The δ is

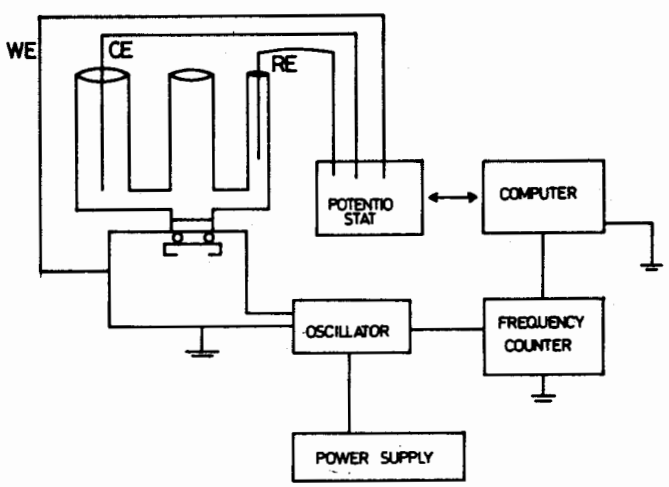

Fig. 2(a): BVD circuit ot describe mechanical properties of a quartz crystal
(b): Circuit to describe the mechanical properties in a liquid

$$\left(\frac{\eta_l}{\pi f_0}\right)^{1/2} P_l \qquad (12)$$

where η_l, P_l are viscosity and density of the liquid. The resonant frequency depends on $[P_l \eta_l]^{1/2}$ as

$$\Delta_f = -f_0^{3/2} \left(\frac{P_l \eta_l}{\pi P_q \mu_q}\right)^{1/2} \qquad (13)$$

Δf = 750 c/s when a QCM is immersed in water and is due to the effective mass of liquid contained in this decay length.

The above equations are derived under 'No slip conditions'. This condition assumes that molecular layer of liquid directly in contact with the vibrating region of the QCM surface moves with the same velocity and amplitude as the vibrating region. The factor $[P_l \eta_l]^{1/2}$ is negligible in air but when the liquid is actually rigid solid [$\eta = \infty$], $(P_l \eta_l)^{1/2}$ is substantial. The acoustic wave will propagate indefinitely and the frequency changes would reflect the true thickness of the solid. If the thickness of this rigid film was large, crystal oscillation would be sufficient because of the significant damping by the large mass; It is this decay of shear wave in liquids that enables operation of QCM & EQCM in liquids.

The changes in and with temperature affect the resonant frequency. The AT-cut crystal is popular because of its zero temperature coefficient at room temperature. When crystals are immersed in solution much larger changes in f_0 with temperature occur due to the coupling of the acoustic shear wave into the solution. f_0 is proportional to $[P_l \eta_l]^{1/2}$.

At 293 K, the is 0.99823 g/c.c, is 1.002 x 10^{-2} g/cm/s and at 298 K the is 0.99707 g/c.c, is 0.8904 x 10^{-12} g/cm/s. Results the f_0 = 41 c/s. This value is larger than those for monolayer adsorption / desorption processes and not negligible with respect to those for solvent on ionic transport in thin films.

Quartz crystals for EQCM

A thin [2-5 nM] adhesion layer of either Cr or Si is usually deposited directly onto the quartz crystal to aid adhesion of the metal electrode. Gold electrodes have been the most commonly used in EQCM studies because of the ease with which gold is evaporated; however Copper, Platinum, Nickel and other metals are also used. In principle any type of material which can be deposited onto

the surface of the underlying metal electrode either by electrodeposition or from vacuum can be used. The only limitation is that the deposition temperature does not exceed 573 K and above which alpha quartz loses piezo electricity [14]. The electrodes become a part of the composite resonator and any change in mass will be reflected in decrease in frequency. When the electrodes become delaminated due to poor adhesion of the underlying, large, discontinuous changes in frequency occur which render a particular useless.

These electrodes are cheap and convenient to reuse them. They can be renewed by vacuum evaporation, sputtering and thermal techniques. Reproducibility is achieved only when they are prepared under extremely clean condition. Cheap rough surfaces cause irreproducibility in oscillations. Over tone polished surfaces are preferred.

Electrochemical cell and experimentation

Electrodes [the diameters of 0.5 to 1 inch approximately] are mounted to the glass cylindrical tube which acts as a working electrode compartment of the 3 - electrodes cell assembly [Fig. 3]. The crystal is mounted so that one of the sides is facing the solution, the opposite electrode facing air. Crystals are mounted either between O- rings or with epoxy, the former being more convenient as the crystals can be easily mounted for reuse or further studies. The two excitation electrodes are electrically connected to an oscillator circuit that contains a broad band RF amplifier so that the electrode facing solution is at hard ground. Usually the circuit is designed so that the crystal is in a feed back loop, therefore driving the crystal at a frequency at which the maximum current can be sustained in a zero phase angle condition; The output of an oscillator is then connected to a conventional frequency meter for measurement. A computer is used to collect frequency and electrochemical data simultaneously as well as to control the wave form applied to the working electrode. This enables simultaneous measurement of electrochemical charge, current voltage and EQCM frequency. The time constant of QCM resonator is fixed by

For a 5 MHZ QCM, it is 1000 and the maximum sampling time is in the milli second range. Frequency counters are capable of sampling the frequency output of the oscillator at 100 milli sec intervals.

Electrochemical parameters

The charge [Q] and the current [i] are compared to F.

$\Delta f = 10^6$ M C f Q/nF where n is the number of electrons transferred to induce deposition; F is the Faraday's constant, M is the apparent molecular weight of the depositing species, C_f is the sensitivity factor for the crystal; 10^6 is used for converting micro gram to grams.

$$I = \frac{d\frac{\Delta f}{dE}(10^{-6}\, nvF)}{MC_f} \qquad (14)$$

in which $[d(\Delta f)/ dE]$ is the derivative of Δf with respect to potential, v is the scan rate, the factor 10 provides for unit conversion. For example, 5 MHZ resonant frequency provides a sensitivity of 0.057 c/s/Sq.cm/nG. The EQCM can detect approximately 10 nG/sq.cm equivalent to 10% of a monolayer of Pb atoms. Above 10 MHZ, the quartz crystals generally become fragile. The successful operation of an EQCM that employed crystals with f_0 = 30 MHZ in which the crystals were prepared by chemical etching of a AT-cur crystals disk. This treatment affords a very thin 50 micro meter thick quartz membrane in the centre of a thick outer quartz ring, the outer ring providing improved stability.

Factors affecting the accuracy

The viscosity of liquid and the deposit affect the frequency. The Sauerbery equation assumes that the frequency shift resulting from a localised deposit is equivalent to the contribution of that deposit when it is portion of a thin film of identical thickness distributed over the entire active QCM area. The generalised equation that

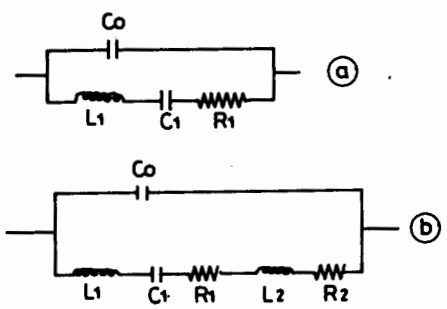

Fig. 3: Schmatic diagram of typical EQCM using Wenking potentiostat

accounts for localised or non uniform mass deposit covering the QCM electrode is also known.

Viscoleastic behaviour of the deposit does not allow the linear mass-frequency relationship in most cases [15]. At MHZ frequencies, the polymer films will tend to have values for u lower than that for quartz due to their lower stiffness,, while having values for higher than that for quartz due to the possibility of viscous loss from translational motion of the chains relative to one another. Since μ increases and decreases below the glass transition temperature [T_g], a knowledge of the Tg for the film material will be useful in gauging whether or not viscoelasticity in the deposit is influencing the resonant frequency of the EQM.

The method based on the dependence of the crystal Q on the viscosity of the deposit may be useful. As Q decreases due to increasing deposit viscosity, the width of the Q vs f plot will increase above the value which arises from immersion of the bare crystal in solution. The presence of detectable increase in Q [e.g. > 10%] should give rise to the suspicion that such deviations might arise. For example Q value for the crystal in liquid is 1000 while loaded with film is 100. The roughness of the deposit can cause large apparent mass loadings due to the liquid trapped in the pores. Error may arise due to the increase in mass due to the liquid trapped in the pores and due to the deposit itself resulting in large decreases in frequency. It is possible to detect the pore volume from frequency measurements. This is done from measuring the difference in the oscillation frequency measurements. This is done from measuring the difference in the oscillation frequency of the crystal coated with dry film in air and with the hydrated crystal in solution. However for a highly porous films the above analysis may not be applicable.

Application to corrosion science — Oxidation

The adsorption of oxygen on gold electrodes was studied [16]. The frequency decrease was 15 c/s with a signal to noise ratio of 50. The frequency changes were reversible in the sense that the original frequency was reattained when the adsorbed layer was removed by reduction. The agreement between the mass change predicted from the charge measurements and that inferred from the frequency change was better than 10%. Hysteres is between the time of passage of electrochemical charge and the observed mass change (i.e. 40$ of the charge of a monolayer was passed before any mass change occurred). This result supported the place exchange mechanism for oxyzen electrosorption.

While studying the formation of chemisorbed oxide layers on gold, the observed mass gain coincided with formation of the oxide layer. However roughening caused the decrease of frequency larger than expected decrease in basic and neutral media [17]. The frequency decrease was smaller H_2SO_4 solution than expected.

The above studies revealed that place exchange mechanism occurs in basic and neutral media with monolayer discharge in acid perhaps accompanied by deprotonation of water [18]. The growth of oxides on copper, gold and silver electrodes [19] enabled to determine the stoichiometry of the oxides. The frequency responses were consistent with the morphology changes of the electrode surfaces. These studies gave an unsight into the surface roughness.

Anodic dissolution

The dissolution of silver in thiurea solution was observed only in presence of dissolved oxygen. Removal of dissolved oxygen by argon caused no dissolution [20]. The oxidation of silver in the presence of 4-4 biphyridly (Bpy) was studied by EQCM. A monovalent silver-Bpy complex was formed. The observed mass changes are found to result from the superposition of a mass loss (from release of Ag^+ ion) and a mass gain (from complex formation) [21]. The influence of illumination on the dissolution between the frequency data obtained in both aerated and deaerated solutions [22].

Investigations of nickel dissolution in H_2SO_4 solution have bene performed using EQCM. The final products in the two active dissolution regions are Ni(II) and that of Ni(III) dissolution ratio to the total anodic charge in the transpassive regions is smaller than that in the two active dissolution regions [23]. The anodic dissolution of nickel films revealed two maxima in the frequency in the frequency vs potential plots indicating a potential dependent dissolution of α and β phases NiH_x. The anodic dissolution of Ni-P film revealed that two different Ni-P compositions were present in the film prior to dissolution [24]. The electrochemical techniques like cyclic voltammetry, anodic stripping voltammetry, coulometry in conjunction with EQCM was used to study the dissolution of copper, nickel and Cu/Ni alloy film formed on polycrystalline gold [26]. The electrochemical

dissolution of copper films in deoxygenated H_2SO_4 solutions revealed that the dissolution rate was linearly dependent on $[O_2]$ and (H^+) ions concentrations enabling to conclude that a heterogeneous surface reaction was operative [26].

Inhibition

In 0.1 *M* $HClO_4$ solutions, the corrosion inhibition of nickel was studied. Acridine, benzyl quinolium chloride, dodecyl quinolinium bromide (DDQBr), tributyl benzyl ammonium iodide and potassium iodide were used as inhibitors and DDQBr was found to be the best [27].

The inhibiting effects of BTA, tolyltriazole and carboxy benzotriazole (CBT) for copper in PH_3 in presence of K1. Only BTA forms three dimensional layers on copper [29]. The BTA-1, TTA, TTA-1 and TTA-1, CBT films were found to have a pronounced continuing effect and are of the order of a few molecular layers. The effect of benzotriazole 2- mercaptobenzothiazole, thiourea and potassium ethyl xanthate on the corrosion of copper form composite polypyrrole/polystyrene sulphonate, copper materials was examined in 0.1 *M* NaCl solutions containing Fe(III) [29]. 5 mercapto-1-phenyl-tetrazole (5 McPhTT) was studied as inhibitor for copper dissolution in 0.1 *M* Na_2SO_4 solution. EQCM data revealed that the addition of the inhibitor to th aggressive solution did not a use a continuous increase in the mass. It was suggested that copper corrosion was hindered by the addition of 5 McPhTT of a mono molecular layer [30]. The frequency shift of EQCM during the corrosion process was simultaneously recorded during the polarisation process and directly related to the mass change of the copper in 0.5 *M* NaCl solution. Benzotriazole and benzoic acid were found to be effective inhibitors [32].

Vapour phase inhibition

The condensation of methyl trimethoxy silane (MTMS) forming a polysiloxane film was studied. Fig. 4 describes the adsorption isotherm for the formation of methyl poly siloxane in humid atmosphere. The addition of MTMS to the gas phase resulted in a negative shift indicating the adsorption of 0.5 of a monolayer of MTMS. I increase of RH from 15% to 80%, a sharp frequency drop was observed resulting from the adsorption of about 3 monolayers of water. Assuming full condensation, the frequency shift would correspond to approximately 6 monolayers of methyl poly siloxane. The sequence of addition of the two compounds water and silane has proved to be important for the rate of film formation. The adsorption of amine, water and butyl trimethoxy silane (BTMS) on iron was studied [32]. at first about 0.5 of a monolayer of BTMS was adsorbed on to iron surface. Then n-propyl amine (PA) was added to the gas phase which resulted in an adsorption of 2.5 monolayers of n-PA. A stable state was now obtained which indicated that the organosilane did not react with the amine in the absence of water. In the next step, the RH was increased. After adsorption of 6 monolayers of water hydrolysis of the silane and condensation of the silanol started and thus a distinct decrease in the frequency was observed. To distinguish the amount of reversibly adsorbed water from the amount of polymer that was formed, the RH was modulated between 80% to 15%. The frequency shifts were due to the desorption and adsorption of water. The final film thickness was about 13 monolayers. Humidity modulations revealed that the amount of reversibly adsorbed water was constant where as the polymer showed constant film growth. The solubility of water decreased with film thickness. The film growth was constant and was about 6 times faster than in the absence of the amine.

The corrosion behaviour of polysiloxane-modified iron surfaces had been studied in a highly corrosive atmosphere [30 ppm SO_2/synthetic

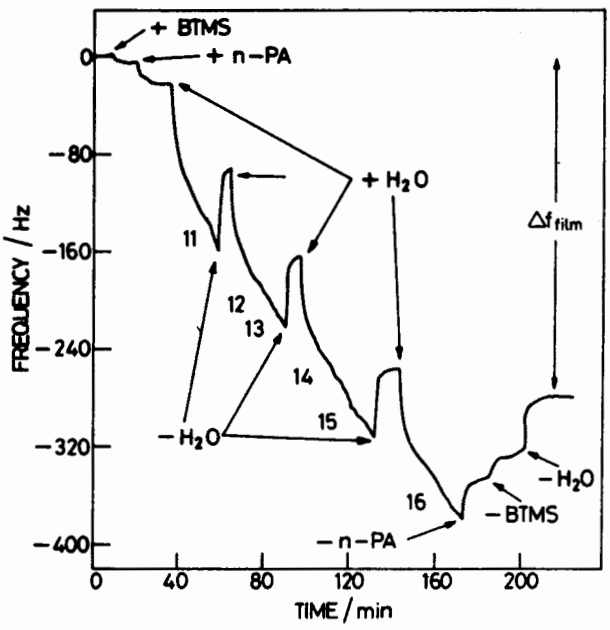

Fig. 4: Adsorption isotherm in the system H_2O/ MTMS (+) addition of MTMS and water (-) exclusion of water

air/80% RH]. The corrosion ate was measured by a quartz crystal microbalance. If the iron surface corrodes,

$$2Fe + \frac{3}{2}O_2 + H_2O \longrightarrow 2FeOOH \quad (15)$$

The frequency change is

$$\Delta f = \frac{-C_f}{A} (\Delta n_{Fe}) M_{(OOH)} \quad (16)$$

$$\text{and the corrosion rate is } I_{corr} = 2Fd \frac{(\Delta n_{Fe})}{dt} \quad (17)$$

$$= \frac{-2FAd \frac{(\Delta f)}{dt}}{cfM_{(OOH)}} \quad (18)$$

where Δn_e is the amount of corroded metallic iron; M(OOH) is the molar mass of the OOH group responsible for the mass gain during corrosion [g/mol]; A s the area of he sample [sq.cm]; F is 96485 C/mol; 2 is the number of electrons transferred; d $(\Delta f)/$ dt is the rate of change of the resonance frequency; C_f is the sensitivity constant [2.26 x 10^8 sq.cm Hz/g].

Fig. 5 presents the resonance frequency as a function of time fro and unmodified iron surface and an iron surface coated with 12 monolayers of mehtyl polysiloxae in corrosive atmospheres. At the beginning the atmosphere was dry synthetic air with 30 ppm SO_2. In the case of the unmodified specimen, a sudden change in the resonance frequency which was due to the adsorption of about 7 monolayers of water. This was followed by a further decrease of the resonance frequency mainly due to corrosion. The corrosion kinetics of iron coated with polysiloxane is characterised by an induction time that depends on the film thickness. In the above example, after an introduction time of about 70 min, the slow decrease of the frequency was due to the start of the corrosion process.

Applications to corrosion engineering

Various surface modification procedures are involved to prepare a galvanised steel to accept an organic coating. A typical reaction sequence is alkaline cleaning of the oxidised and contaminated surface, rinsing then either chromating and rinsing or activation in a colloidal solution of titanyl phosphate followed by a phosphating process. To simulate the complex industrial process of e.. phosphating of zinc coated steel, a system was built that was capable of investigating different processes in real time with EQCM [33].

Cleaning

The transient of the resonance frequency during the sequence of rinsing, alkaline cleaning, rinsing, chromating and rinsing was taken. In order to differentiate between the chemical dissolution reaction and the anodic dissolution of zinc, the oxygen activity was changed in the alkaline cleaning solution. XPS studies on the zinc quartz crystals confirmed that the surface of zinc should always be covered by a thin layer of $Zn(OH)_2$ and these fluxes of zincate and OH^- ions were compared. The diffusion of OH^- ion was always much larger than the outward diffusion zincate.

Chromating

From an industrial chromating solution for the coil coating industry on an electrogalvanised zinc *in situ* EQCM studies were carried. From the changes in frequency time curve, the sequences of events for 2 arrests were understood as

Region I

$$ZnO + 2H^+ \longrightarrow Zn^{2+} + H_2O \text{ or} \quad (19)$$

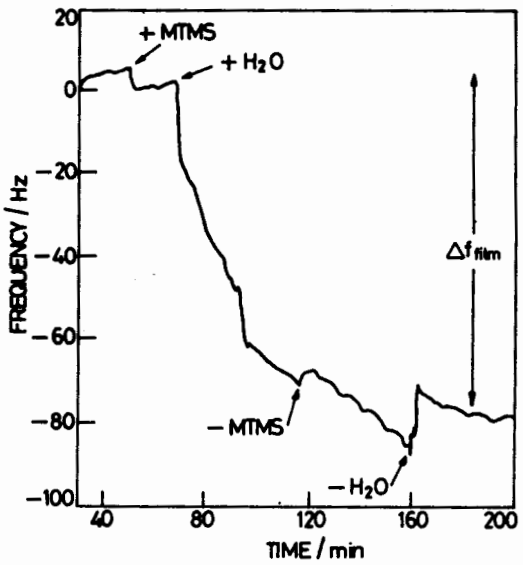

Fig. 5: Adsorption isotherm in the system BTMS + nPA
(+) addition of BTMS, nPA, H_2O
(-) exclusion of nPA, BTMS, H_2O
t_1, t_2, t_3, t_4, ... from the IR spectra measured time intervals (see ref 22)

$$Zn + 2H^+ \longrightarrow Zn^{2+} + H_2 \quad (20)$$

Region II: The chromating process as

$$2CrO_4^{2-} + 3H_2O + 10H^+ \longrightarrow 2Cr^{3+} + 8H_2O \quad (21)$$

$$Cr^{3+} + 12H_2O \longrightarrow 2\,[Cr\,(H_2O)_{12}]^{3+} \quad (22)$$

and

$$2\,[Cr\,(H_2O)_{12}]^{3+} \longrightarrow \left[(H_2O)_4\ Cr \begin{matrix} H \\ O \\ \\ O \\ H \end{matrix} Cr\,(H_2O)_4 \right]^{4+}$$

$$+ 2H_2O + 2H^+ \quad (23)$$

Phosphating

For an electrogalvanised zinc quartz crystal during zinc phosphation, mass and potential transients were obtained. Three distinct regions were observed in the mass changes transients. In the first region, dissolution of zinc over compensated the precipitation of hoepite. In the second region (after 5 seconds) the growth of hoepite became dominant and Δf decreased. In the last region the mass transient reached a maximum of 2.5 g/m^2 similar to that obtained in the technological process.

CONCLUSION

EQCM has become a versatile tool to follow the various phenomenon like oxidation, chemical dissolution, passive dissolution, inhibition. In the technological processes involving surface engineering EQCM throws more light on the chemical events occurring during the chromating and phosphating. The low cost and simplicity make this tool attractive. The high precision of the measurement of changes in frequency and impedance parameters make the EQCM a promising tool to understand surface chemistry.

REFERENCES

1. P Curie and J Curie, *CR Acad Sci*, **91** (1880) 294
2. V G Bottom, *Introduction to quartz crystal unit design*, Van Nonstrand Reinhold, New York (1982)
3. D Sa,t Hy-Q-hand book of quartz crystal devices, Van Nonstrand Reinhold, Bershie, England (1987)
4. R D Mindlin, *Q Appl math*, **19** (1951) 51
5. H Bahadur and R Parshad, *in physical acoustics*, Vol 16 (W P Mason and R N Thurston) (Eds) Academic Press, New York (1982) 37-171
6. H K Pulker and W Shadler, *Nuovocimento* **57B** (1972) 4385
7. G Sauerbury, *Z Phys*, **178** (1964) 457
8. C S Lu and O Lewis, *J Appl Phys*, **43** (1972) 4385
9. W P Mason, *Electrochemical transducers and wave filters*, Van Nostrand, New York, (1948)
10. W C Cady, *Piezoelectricity*, Dover, New York (1964)
11. L V Rajakovic, B A Cavic-Vlasak, V Ghaemmaghami, K M R Kallury, A L Kipling and M Thompson, *Anal Chem*, **63** (1991) 615
12. A L Kipling and M Thompson, *Anal Chem*, **62** (1990) 1514
13. W S tockel and Schumacher, *Ber Bunsenges Phys Chem*, **345** (1987) 91
14. C Lu and A W Zanderna (Eds), *Applications of piezoelectric quartz crystal microbalance, Methods and phenomena*, Vol 17, Elsevier Science Publishing, New York (1984)
15. J D Ferry, *Viscoelastic properties of polymers*, wiley Interscience, New York (1980)
16. S Brukenstien and M Shay, *J Electroanal Chem*, **188** (1985) 131
17. R Schmacher, G Borges and K K Kanazawa, *Surf Sci*, **163L** (1985) 621
18. W Stockel and R Schumacher, *Ber Bunsenges Chem*, **91** (1987) 345
19. M Benje, U Hoffmann, U Pitterman and K G Weil, *Ber Bunsenges Phys Chem*, **92** (1988) 1257
20. C G Chen, X H Guo, G H Zhang and Z Q Huang, *193rd Electrochemical Society Meeting*, Spring (1998) San Diego, California, Vol 98-1, abstract no 139.
21. C Paul Wilde and Devi Pisharoai, *J Electroanal Chem*, **398** (1995) 143
22. E Juzellunas, P Kalinauskas and P Miecinskas, *J Electrochem Soc*, **143(5)** (1996) 1525
23. M Itagaki, H Nakazawa, K Watanabe and K Noda, *Corros Sci*, **39(5)** (1997) 901
24. M Benje, M Eiermann, U Pittermann and K G Weil, *Ber Bunsenges Phys Chem*, **92** (1988) 1257
25. M Zhou, N Myung, X Chen and K Rajeshwar, *J Electroanal Chem*, **398** (1995) 5
26. R Schumacher, A Muller and W Stockel, *J Electroanal Chem*, **219** (1987) 311
27. F Zuochi, M Fonsati and G Trabanelli, *J Appl Electrochem*, **28** (1998) 441
28. Dirk Jope, Joachion Sell, Howard W Pickering and Konrad G Weil, *J Electrochem Soc*, **142(7)** (1995) 2170
29. Maria Hepel, *191st Electrochemical Society Spring*, (1997) Montreal Quebec, Canada, Abstract No 230
30. E Szocs, Gy Vazstag, A Shaban, G Konczos and E Kalman, *J Appl Electfochem*, **29** (1999) 1339
31. An Hong Zhou, Bin Xie and Nai Xian Xie, *Corros Sci*, **42** (2000) 469
32. Martin Startmann, Wolfrum Furbeth, Guido Gruna Meier, Reinherd Losch and Cedric Reinartz, *in Corrosion Mechanisms in Theory and Practice*, (Ed) P Marcus and J Ouder, Marcel Dekker, New York (1995)
33. Karl Heinz, Stellin Berger, Michael Welpers, Thomas Fili, Cedric Reinartz, Thomas Paul and Martin Startmann, *Faraday Discuss*, **107** (1997) 307